

Solvent-free semihydrogenation of acetylene alcohols in a capillary reactor coated with a Pd–Bi/TiO<sub>2</sub> catalyst

Nikolay Cherkasov a, 1

Alex O. Ibadon a, \*

a.o.ibhadon@hull.ac.uk

zdx@gmx.com

Evgeny V. Rebrov b, c

aCatalysis and Reactor Engineering Research Group, Department of Chemistry and School of Biological, Biomedical and Environmental Sciences, University of Hull, Cottingham Road, Hull HU6 7RX, UK

Catalysis and Reactor Engineering Research Group, Department of Chemistry and School of Biological, Biomedical and Environmental Sciences, University of Hull, Cottingham Road, Hull, HU6 7RX, UK

bSchool of Engineering, University of Warwick, Coventry CV4 7AL, UK

School of Engineering, University of Warwick, Coventry, CV4 7AL, UK

cDepartment of Biotechnology and Chemistry, Tver State Technical University, Tver 170026, Russia

Department of Biotechnology and Chemistry, Tver State Technical University, Tver, 170026, Russia

\*Corresponding author.

1Present address: School of Engineering, University of Warwick, Coventry CV4 7AL, UK.

Abstract

A solvent-free semihydrogenation of 2-methyl-3-butyn-2-ol (MBY) to 2-methyl-3-buten-2-ol was performed in a capillary reactor (10 m long, 0.53 mm i.d.) coated with a titania supported Pd–Bi catalyst. Several coatings with different Pd/Bi ratio have been prepared. The catalysts have been characterized with SEM, TEM, EDX, XRD analysis and N<sub>2</sub> adsorption–desorption measurements. The maximum alkene yield of 90% was obtained at a molar Pd/Bi ratio of 11. The yield was increased to 95% in the presence of 10 mol.% pyridine in the reaction mixture. The alkene selectivity decreased with time due to leaching of Bi. The leaching was fully suppressed in the presence of 1 vol.% acetic acid in the reaction mixture. The catalyst remained stable for 100 h of continuous operation. The results demonstrate that capillary reactors provide alkene selectivity the same compared to ideal stirred tank batch reactors.

Keywords: Semihydrogenation; Acetylene; Pd; Solvent-free

1 Introduction

The conversion of alkynes into alkenes through semihydrogenation reactions is a critical step in the synthesis of many vital fine and speciality chemicals. For example, semihydrogenation reactions are used in the synthesis of a fragrance compound linalool and vitamins K1 and E [1,2]. Other vitamins are industrially produced via semihydrogenation steps at a scale of up to 10,000 tons a year [1–3]. Moreover semihydrogenation reactions are extensively used in the synthesis of many other important fine chemicals including fragrances, agrochemicals, food additives, pharmaceuticals and

others [1,4,5]. In particular, Fig. 1 shows the scheme of hydrogenation reactions of an important industrial intermediate 2-methyl-3-butyn-2-ol (MBY), where along with the target semihydrogenation product, 2-methyl-3-buten-2-ol (MBE), by-product formation is possible via overhydrogenation to MBA or dimerisation to C<sub>10</sub> products. The results presented by Rebrov et al. [6], Yarulin et al. [7], and our previous results [6] show that MBY is a representative example for a large number of acetylene alcohols with 10, 15 or 20 carbon atoms. The kinetics of hydrogenation of dehydrolinalool (C<sub>10</sub>H<sub>16</sub>O, 3,7-dimethyl-6-octaen-1-yne-3-ol) and dehydroisophytol (C<sub>20</sub>H<sub>38</sub>O, 3,7,11,15-tetramethyl-1-hexadecyne-3-ol) follows the same trend while a maximum of selectivity is observed at a slightly different ratio of Pd and second metal in the bimetallic catalyst [6]. Still such minor change could not be considered as significant therefore all results obtained in the hydrogenation of 2-methyl-3-butyn-2-ol can be translated to dehydrolinalool and dehydroisophytol.

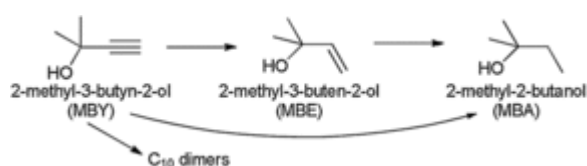


Fig. 1 Scheme of 2-methyl-3-butyn-2-ol hydrogenation.

The state-of-the-art approach to semihydrogenation includes (i) the use of batch or semi-batch reactors, and (ii) application of Pd catalysts partially poisoned with Pb (Lindlar catalyst) or other metals such as Cu, Ag, Bi, Sn, Ga [7–11]. Batch reactors provide quick scaling up from laboratory to industrial scale and they are easily adaptable for various reaction types [12,13]. However, their low energy efficiency, the excessive use of solvents, and the high toxicity of lead compounds in the Lindlar catalyst cause environmental concerns. Moreover, the process optimization is usually required even after minor changes in the substrate molecule structure to maximize the product yield, which is particularly laborious for batch reactors [2]. Not surprisingly, small-scale industrial chemical processes in the pharmaceutical industry produce more than 25 kilograms of waste per kilogram of the product, thus having a very high overall environmental impact [1,14].

An elegant solution to the environmental problems described lies in process intensification which is possible in microreactors [15–18]. Microreactors provide high surface to volume ratio of several orders of magnitude as high as batch reactors, which results in high heat- and mass-transfer rates [19–22]. The high heat transfer rates allow fast heating or cooling of reaction mixture, so highly exothermic hydrogenation reactions can be performed under solvent-free conditions at high rate. In microreactors, the reactions are kinetically controlled, resulting in higher product selectivity. Small reaction volume of microreactors allows safe utilization of high pressure using inexpensive equipment, while laminar flow allows precise control of the residence time [15,19,23]. In addition, continuous operation of microreactors allows simple and quick process optimization resulting in lower labour costs [12,24]. All these advantages result in substantially improved sustainability of chemical processes performed in microreactors [15,22,25,26].

Although microreactors have demonstrated great promise in many organic liquid-phase reactions, application of heterogeneous catalysts for gas–liquid reactions still remains a major challenge [19,27–29]. For example, hydrogenation reactions require an efficient handling of (i) hydrogen gas, (ii) liquid substrate medium, and (iii) solid catalyst to ensure quick mass transfer and reaction rates. Furthermore, semihydrogenation reactions require precise control of the reactant residence time due to the possibility of over-hydrogenation. Therefore, essential requirements for an efficient semihydrogenation in microreactors are (i) a consistent, controllable and very narrow residence time distribution, and (ii) the absence of internal diffusion limitations [30].

There are three ways to perform heterogeneously catalysed multiphase reactions in microreactors: (i) using small catalyst particles in a micro fixed bed configuration [21,31,32], (ii) with magnetically-supported catalysts held at the reactor walls with magnetic field [33–36], or (iii) with a catalytic coating deposited onto the inner reactor walls [6,37–41]. The first approach seems advantageous because any catalyst suitable for batch hydrogenation can be used to make a packed-bed reactor. However, gas–liquid reactions in packed-bed reactors have a number of problems associated with poor heat and mass transfer. In addition, liquid tends to form preferential pathways between the catalyst particles leading to poor radial dispersion and wide residence time distribution, which in the case of semihydrogenation results in low alkene yield [42–44]. Magnetically-recoverable catalysts offer a convenient way of catalyst introduction and good reusability, but the price of the catalysts and complexity of reactor operation seem to be a disadvantage for industrial semihydrogenation at the current stage. Therefore, wall-coated reactors are more suitable because they allow good control of the residence time and provide high heat transfer rates due to an intimate contact between the catalyst and the reactor wall. However, wall-coated reactors are usually more expensive compared to packed-bed systems and require a reproducible deposition method for catalytic coating. In addition, high-performance capillary reactors require high catalyst loading, long reactor channels and thick porous catalytic coatings [6,39]. To the best of our knowledge, capillary reactors reported in the literature for semihydrogenation reactions have a throughput below 5 g of alkynol a day and suffer from solvent overuse [6,39,41,45–47]. In order to address these problems, we have studied a solvent free semihydrogenation of MBY in a capillary reactor coated with a titania supported Pd–Bi catalyst. This catalyst uses Bi as a non-toxic selectivity enhancing agent, which increases alkene semihydrogenation selectivity by preferentially poisoning step sites of Pd particles [8,9].

## 2 Experimental

### 2.1 Synthesis of Pd–Bi/TiO<sub>2</sub> coating

A titanium dioxide sol was prepared by dissolving 7.3 g of titanium (IV) isopropoxide (Sigma–Aldrich, 97 wt.%) in 8 mL methanol (Fisher Chemical, 99.95 wt.%); then 7.0 mL of water was added while stirring. After 2 h of stirring under reflux, 0.7 mL of concentrated HNO<sub>3</sub> (Fisher Scientific, 65 wt.%) was added to disperse possible agglomerates, the sol was refluxed for 2 h followed by the addition of 0.3 g Pluronic F127 (Sigma–Aldrich), and the stirring was continued at room temperature for 12 h.

The dispersion of Pd nanoparticles poisoned with Bi was obtained by dissolving 160 mg of palladium (II) acetate (Sigma–Aldrich, 98 wt.%) and 210 mg polyvinylpyrrolidone (Sigma–Aldrich) in 10.0 mL methanol. The resulting solution was reduced by adding 60 mg sodium borohydride (Sigma–Aldrich, 98% wt.). After stirring for 2 h, sodium borohydride was neutralized with 0.2 mL nitric acid, and a solution of 52 mg of bismuth nitrate pentahydrate (Sigma–Aldrich, 98 wt.%), 0.10 mL nitric acid in 5.0 mL methanol was added. The dispersion was stirred in hydrogen for 1 h to poison Pd nanoparticles with Bi [8,48]. The sol for wall-coating was obtained by mixing 2.3 mL of the TiO<sub>2</sub> sol, 1.0 mL of the Pd–Bi nanoparticle dispersion with methanol to a total volume of 10.0 mL.

A fused silica capillary (10 m × 0.53 mm i.d.) was activated by passing a saturated aqueous NaOH solution for 2 h and then washing with water. The sol containing Pd–Bi/TiO<sub>2</sub> was fed into the capillary using a syringe and then the filling end of the capillary was closed with a valve. Afterwards, the capillary was slowly introduced into an oven (200 °C) using a stepper motor at a displacement speed of 0.2 mm/s. The coating method used provides quick and highly controllable method for solvent evaporation from the precursor sols and minimises capillary clogging [37]. The wall-coated capillary obtained was dried in a vacuum oven at 200 °C for 12 h, washed with hexane and methanol

(100  $\mu\text{L min}^{-1}$  for 1 h each). The mass of the coating was 1.6  $\text{mg m}^{-1}$  with a nominal Pd loading of 2.5 wt.%. Several capillaries were coated during the study and demonstrated catalyst mass reproducibility within  $\pm 7\%$ . A glass tube (3.1 mm o.d., 1.6 mm i.d., 300 mm long) was coated using the same method, the coating was mechanically removed and used for XRD and nitrogen physisorption characterization.

## 2.2 Characterization

The thickness of the catalyst coating on the capillary channels was studied by using a TM-1000 Hitachi tabletop scanning electron microscope (SEM) examining 25 capillary cross-sections of the capillary evenly distributed along the capillary length. Elemental energy-dispersive X-ray (EDX) analysis was performed in a Zeiss EVO SEM studying the coating mechanically removed from the capillary reactor and placed on a conductive adhesive pad. The content of Pd, Bi and Ti was determined averaging the results from 4–6 areas of the powder samples.

Transmission electron microscopy (TEM) study was performed using a Jeol 2010 instrument equipped with an EDX spectrometer produced by Oxford Instruments. For this study, the coating removed from the capillary reactor was applied on carbon-coated copper grids, and 5–8 regions of the grid were studied to obtain representative data.

The surface area and pore size distribution of the coatings were measured by  $\text{N}_2$  adsorption–desorption isotherms (Energas, 99.999 vol.%) using a TriStar 3000 micrometrics analyser using standard multipoint BET analysis and BJH pore distribution methods. Prior to nitrogen adsorption, the catalyst material was dried in a nitrogen flow at 140  $^\circ\text{C}$  for 3 h.

Powder X-ray diffraction (XRD) patterns were recorded using an Empyrean powder X-ray diffractometer equipped with a monochromatic  $\text{K}\alpha$ -Cu X-ray source in the  $2\theta$  range 20–70 $^\circ$ , step size 0.039 $^\circ$  and step time 335 s. The pattern was analysed using a PANalytical Highscore Plus software.

## 2.3 Catalytic test

The coated capillaries obtained were tested in the apparatus schematically presented in Fig. 2. The setup included a continuous flow syringe pump, a pressure transducer, and mass-flow controllers for hydrogen and nitrogen (CK gas, 99.999 vol.%) connected via a one-way valve and a cross-mixer to the capillary reactor [37]. MBY (Sigma–Aldrich, 98 wt.%) was used for the reaction undiluted at the flow range from 10 to 100  $\mu\text{L min}^{-1}$ . The hydrogen flow rate was constant at 10  $\text{mL min}^{-1}$  (STP), and the reaction temperature was changed in the range from 30 to 70  $^\circ\text{C}$  using a thermostat. At each reaction condition studied, the system was allowed to reach steady state within 10–30 min, then 3–5 liquid samples were taken from the reactor outlet, diluted 50:1 with hexane and analysed using a Varian 430 gas chromatograph equipped with an autosampler, a 30 m Stabilwax capillary column and an FID detector.

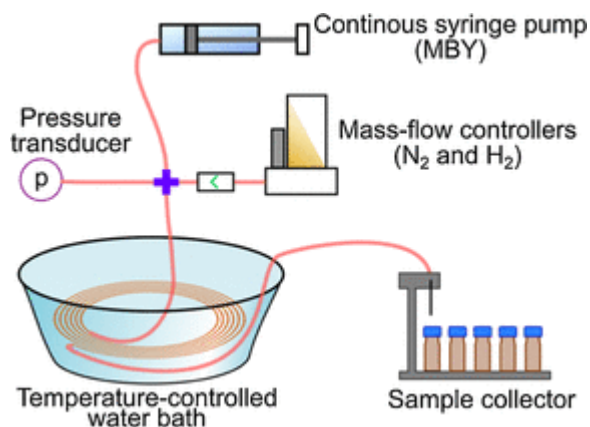


Fig. 2 Scheme of the hydrogenation capillary reactor Schematic view of the capillary reactor.

### 3 Results and discussion

#### 3.1 Characterization of the Pd–Bi/TiO<sub>2</sub> coating

Fig. 3 shows the pore size distribution obtained from the desorption branch of the isotherm and an XRD pattern of the coating obtained. It can be seen that the coating is mesoporous with an average pore diameter of 2.6 nm and a specific surface area of 180 m<sup>2</sup> g<sup>-1</sup>. The XRD pattern shows that the coating consists of anatase and brookite phases in a 40:60 ratio. These results are similar to our previous study [37], where a titania sol with a higher concentration was obtained from a titanium butoxide precursor rather than titanium isopropoxide. In addition, the coating morphology is similar to that reported by Bleta et al. [49] who obtained TiO<sub>2</sub> powders by drying titania sols. These data suggest that the coating morphology can be tuned using the procedures reported for sol drying [49,50].

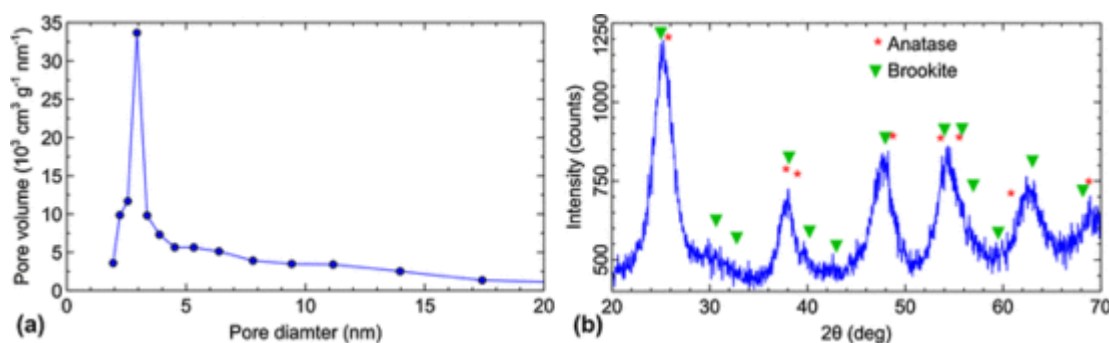


Fig. 3 (a) Pore size distribution and (b) PXRD pattern of Pd–Bi/TiO<sub>2</sub> coating obtained in a 1.6 mm glass tube.

A representative SEM image of the coated capillary is shown in Fig. 4a. Statistical analysis of the coating thickness obtained by studying cross-sectional SEM images (Fig. 4b) shows that a uniform coating was obtained with an average thickness of 2.0 μm and the standard deviation of 1.0 μm. The TEM study showed that Pd–Bi particles were 4–10 nm in diameter (Fig. 4c). The Pd content determined by EDX analysis was 2.8 ± 0.3 wt.%, which is in good agreement with the nominal Pd loading of 2.5 wt.%. However, the Bi content was 0.5 ± 0.2 wt.% corresponding to a Pd/Bi molar ratio of about 11. Because large amount of the material was needed for ICP analysis (10 mg), it was performed only for the sample obtained in a 1.6 mm id glass tube. The obtained results, a Pd loading of 2.55 wt.% and a Bi loading of 0.32 wt.%, showed excellent agreement with EDX data obtained for a sample obtained from the capillary reactor. The observed Pd/Bi ratio was substantially higher than

Pd/Bi precursor ratio used of 7, which suggest that only a partial reduction of Bi ions occurred in a methanol solution as opposed their complete reduction in an aqueous solution [9,37]. This effect can be explained by the change in electrode potential of the  $\text{Bi}^{3+}/\text{Bi}^0$  system in a non-aqueous solvent [51,52].

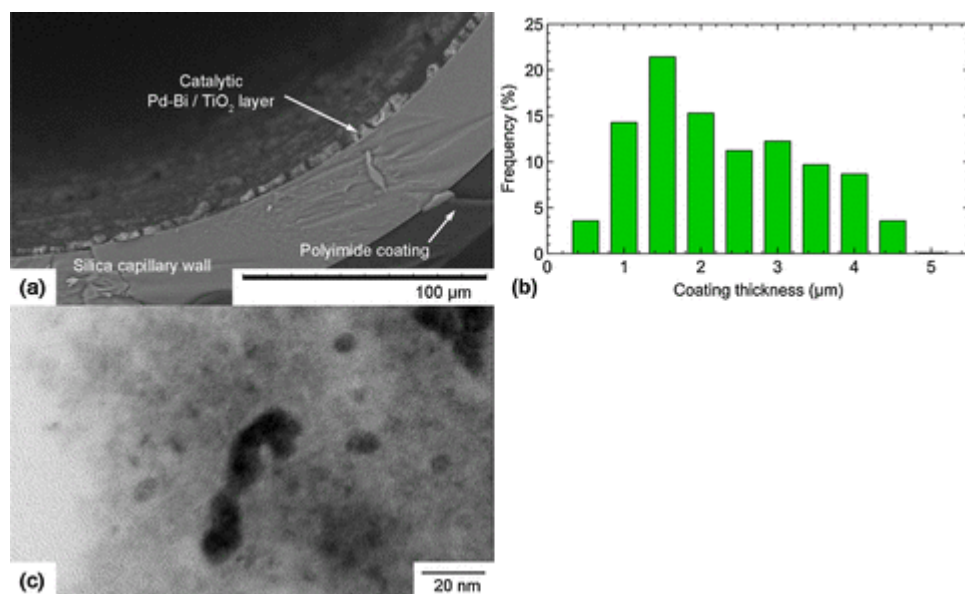


Fig. 4 (a) SEM image of the Pd–Bi/TiO<sub>2</sub> wall-coated capillary, (b) axial coating thickness distribution obtained from 25 cross-sectional SEM images, and (c) TEM image of the Pd–Bi nanoparticles.

### 3.2 Flow regimes in the capillary reactor

The solvent-free alkyne hydrogenation of MBY into MBE is accompanied by very high hydrogen consumption. For example, the conversion of 1 μL of the reactant requires about 230 μL (STP) of hydrogen. Hence, the hydrogen flow rate should be more than 2 orders of magnitude higher than the liquid flow rate to provide stoichiometric reactant ratio in high throughput hydrogenation reactors. Moreover, as a result of high hydrogen consumption, a flow regime can change inside the microreactor [53]. Therefore it is necessary to obtain the flow regime map corresponding to selected experimental conditions.

The flow regimes were studied observing flows of hydrogen and MBY coloured with methylene blue in an untreated silica capillary with an internal diameter of 0.53 mm using an optical microscope (Fig. 5). Several flow regimes were observed in the studied range of gas and liquid flow rates. At the reactor inlet, a slug-annular regime was always observed under the studied flow conditions. The flow changed to a slug flow regime when the hydrogen flow rate decreased to 1–4 mL min<sup>-1</sup>. For higher gas flow rates above 20 mL min<sup>-1</sup>, an annular flow regime was realised. A bubbly flow regime was not observed as small gas bubbles are quickly consumed in the hydrogenation reaction forming a single phase (liquid) flow [42,54,55]. A single phase liquid flow was observed in the case of full hydrogen consumption.

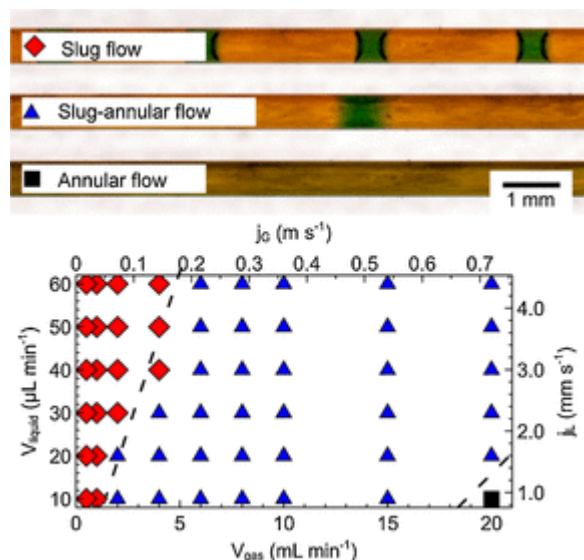


Fig. 5 Images of hydrogen-MBY (coloured with methylene blue) two phase flow regimes; and an experimental flow regime map for hydrogen (atmospheric pressure)—MBY in the capillary with 0.53 mm i.d.,  $j_G$  and  $j_L$  are superficial liquid and gas velocities, respectively.

### 3.3 Solvent-free semihydrogenation of MBY

Fig. 6a shows the effect of the reaction temperature and liquid flow rate on conversion in the solvent-free semihydrogenation of MBY performed in a 10 m capillary reactor coated with a Pd–Bi/TiO<sub>2</sub> catalyst. At a constant reaction temperature, the MBY conversion decreased at higher liquid flow rates due to lower residence time, while the MBE selectivity increased up to 94% in the entire range of temperatures studied (Fig. 6b). An increase in alkene selectivity at low alkyne conversions is typical for Pd-based catalysts and is explained by the high adsorption energy of alkyne molecules. This results in the displacement of alkene molecules from the catalyst surface and prevents overhydrogenation to alkanes [56,57]. However in a hexane solution, the maximum MBE selectivity reached almost 98% [9,37]. The lower selectivity observed in the capillary reactor was caused by lower Bi content due to incomplete Bi reduction from the methanol solution as it was discussed above.

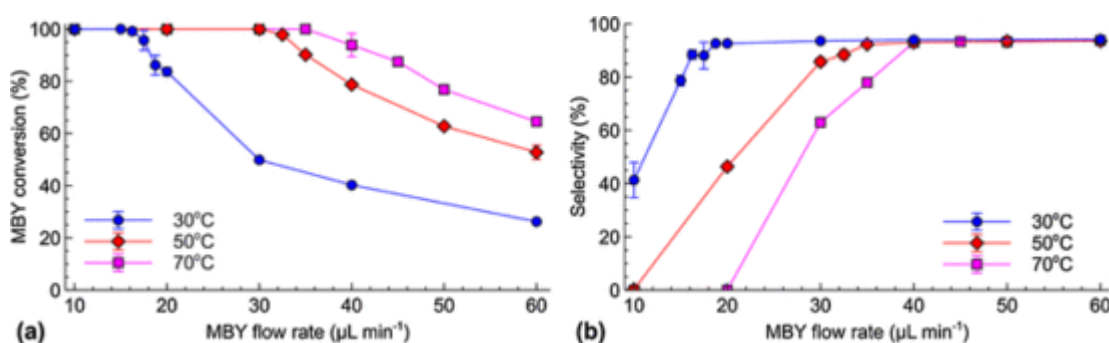


Fig. 6 (a) MBY conversion and (b) MBE selectivity as a function of MBY flow rate in solvent-free MBY hydrogenation in a Pd–Bi/TiO<sub>2</sub>-coated capillary reactor at a hydrogen flow of 10 mL min<sup>-1</sup> and different reaction temperatures.

The fluctuations in the MBY conversion and MBE selectivity observed in a 10 m capillary reactor were smaller (Fig. 6), as compared with those of  $\pm 4\%$  in a 2.5 m long reactor [37]. These discrepancies can be explained by fluctuations in the reaction temperature, reactant flow rates, and

more importantly, the pressure drop changes as a result of transition between hydrodynamic regimes in the capillary reactor. It appears that a longer reactor length significantly decreases the pressure fluctuations [58].

The MBE yield as a function of MBY flow rate at different reaction temperatures is shown in Fig. 7a. At every reaction temperature, a maximum MBE yield of 87–90% was observed at the MBY flow rate corresponding to the MBY conversion of 92–98%. An increase or decrease in the MBY flow rate provided a lower MBE yield as a result of either decreased conversion or over-hydrogenation. However, no products other than MBE and MBA were identified, which shows zero selectivity towards oligomerization. More importantly, the reactor throughput increased with the reaction temperature allowing the MBE production capacity of 40  $\mu\text{L min}^{-1}$  (or about 50 g day $^{-1}$ ) with the MBE yield of up to 90% in a single 10 m capillary reactor.

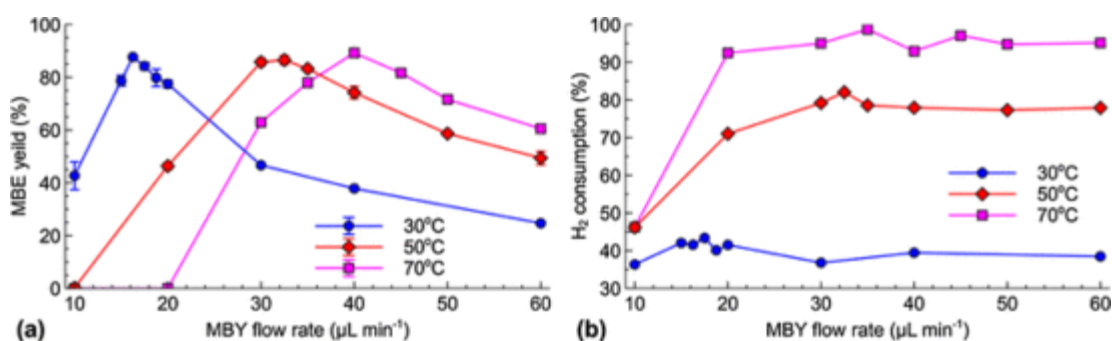


Fig. 7 (a) MBE yield and (b) hydrogen consumption as a function of MBY flow rate in solvent-free MBY hydrogenation in a Pd–Bi/TiO<sub>2</sub>-coated capillary reactor at a hydrogen flow of 10 mL min $^{-1}$  and different reaction temperatures.

The hydrogen conversion notably increased with the temperature due to increased reaction rate (Fig. 7b). As the temperature increased from 30 to 70 °C, the hydrogen conversion increased from 45 to 80% and the slug-annular flow was transformed to the slug flow regime near the reactor outlet (Fig. 5).

### 3.4 MBY semihydrogenation in the presence of pyridine

An addition of competitive adsorbates such as quinoline or pyridine is a common way to increase selectivity towards alkene in a hydrogenation reaction. These molecules, being adsorbed on the catalyst surface, isolate Pd active sites, and decrease the heat of adsorption of semihydrogenated alkene species [59]. This increases alkene selectivity, often up to 99%, via the reduced rate of formation of over-hydrogenation products, although the alkyne hydrogenation rate also decreases [30,39].

The effect of pyridine addition on the MBY conversion and MBE selectivity was studied by addition of 1 and 10 mol.% pyridine solutions to the reactant solution at 70 °C (Fig. 8). A full MBY conversion was observed up to a liquid flow rate of 33  $\mu\text{L min}^{-1}$  in the absence of pyridine. An addition of 1 and 10 mol.% pyridine reduced conversion to 95 and 90%, respectively, due to the blocking of the active sites [39,60]. The MBE selectivity increased up to 98% in the presence of pyridine (Fig. 8b). The MBY conversion over the Pd–Bi/TiO<sub>2</sub> catalyst decreased by 5% and the MBE selectivity increased by 1.5% in the presence of high concentration of pyridine (10 mol.%) as compared with the low concentration case (1 mol.%). This change is relatively low as compared to our previous study [39], where we observed a 4% increase in the MBE selectivity on addition of pyridine to an MBY methanol solution. In the present study, the MBY concentration was more than 3 orders of magnitude higher

than that in our previous study [39]. This results in the preferential occupation of catalyst active sites with MBY even in the presence of pyridine. On the contrary, in a highly diluted solution, Nijhuis et al. [30] observed a twentyfold decrease in the alkene hydrogenation rate on introduction of 20 mM quinoline, while 200 mM quinoline fully suppressed the alkene overhydrogenation reaction.

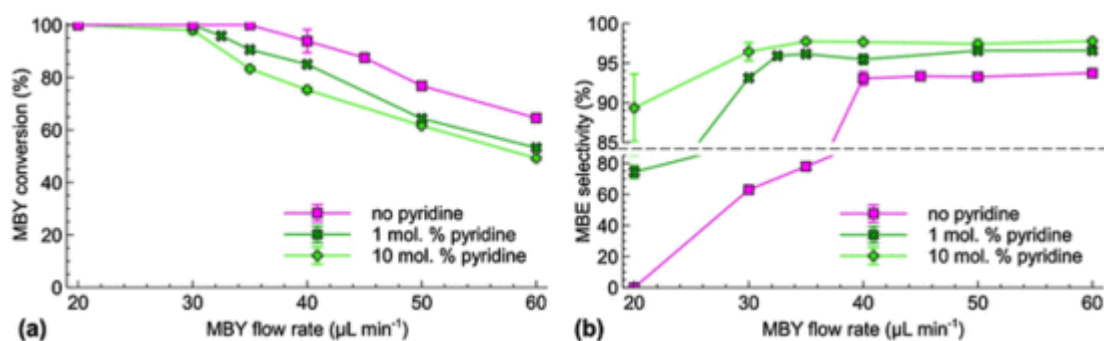


Fig. 8 (a) MBY conversion and (b) MBE selectivity as a function of liquid flow rate in MBY hydrogenation in the presence of pyridine in a Pd–Bi/TiO<sub>2</sub>-coated capillary reactor at a 10 mL/min hydrogen flow rate.

In the presence of the high and low concentrations of pyridine, the MBE yield increased to 95 and 93%, respectively. However, the reactor throughput decreased from 50 to 35 g day<sup>-1</sup> due to the decreased reaction rate (Fig. 9a). The reaction temperature has no effect on the MBE selectivity over the Pd–Bi/TiO<sub>2</sub> catalyst in the absence of pyridine (Fig. 9b). It can be concluded that the changes in flow regimes and associated changes in the mass transfer rates do not influence alkene selectivity [53].

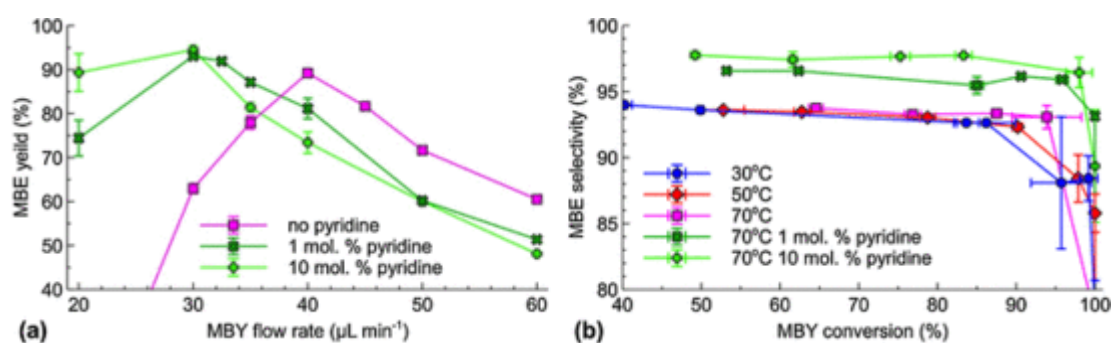


Fig. 9 (a) MBE yield as a function of liquid flow rate in MBY hydrogenation in the presence of pyridine over a Pd–Bi/TiO<sub>2</sub>-coated capillary reactor at a 10 mL/min hydrogen flow rate, and (b) MBY conversion vs. MBE selectivity plot for the studied reaction conditions.

### 3.5 Deactivation of the Pd–Bi/TiO<sub>2</sub> catalyst

The MBY semihydrogenation can efficiently be performed without a solvent with a throughput of 50 g day<sup>-1</sup> in a 10 m long capillary reactor coated with a Pd–Bi/TiO<sub>2</sub> catalyst. However, long-term stability is an essential requirement for the application of capillary reactors in industrial production. To study the long term stability of the Pd–Bi/TiO<sub>2</sub> coating, a 2 m capillary reactor (0.53 mm i.d.) was wall-coated with a titania supported Pd–Bi catalyst with a Pd/Bi molar ratio of 7 and a Pd loading of 3.4 wt.% using the previously reported method [37]. The catalyst with increased Bi content (Pd/Bi molar ratio of 7) was chosen for this study aiming to increase MBE selectivity without the addition of pyridine.

Fig. 10 shows the performance of this capillary reactor in the solvent-free hydrogenation of MBY for 100 h. The initial MBE selectivity was above 98%, which is by 4% higher than that obtained over the Pd–Bi catalyst with a Pd/Bi molar ratio of 11 (Fig. 9b). Moreover, the same 98% MBE selectivity was obtained using a 0.12 M MBY solution in hexane [9]. This shows that the catalyst behaviour is identical in the semihydrogenation in a hexane solution and under solvent-free conditions. Similar behaviour was observed over Pd/ZnO catalysts in diluted solutions and solvent-free conditions [61,62]. This can be explained by the fact that supported Pd catalysts have very high heat of adsorption of alkyne species, which leads to the full coverage of Pd sites with MBY molecules even at relatively low MBY concentrations [63].

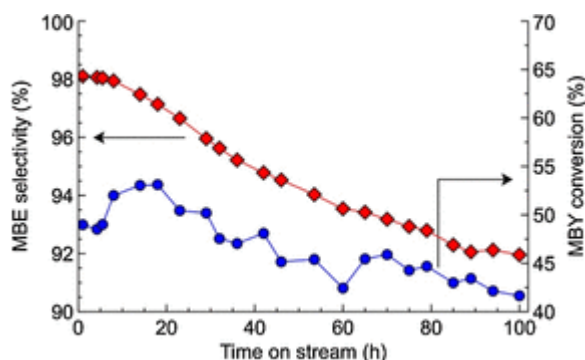


Fig. 10 MBY conversion and MBE selectivity over a Pd–Bi/TiO<sub>2</sub> coating in a 2 m capillary (0.53 mm i.d.) in solvent-free MBY hydrogenation. Pd loading in the coating is 3.4 wt.%, Pd/Bi molar ratio is 7. MBY flow rate is 20  $\mu\text{L min}^{-1}$ , hydrogen flow rate is 5  $\text{mL min}^{-1}$  (STP), temperature is 50  $^{\circ}\text{C}$ , ambient pressure, 0.2 bar pressure drop.

A constant MBE selectivity of 98% was observed in the first 10 h of operation (Fig. 10). However within the next 80 h, it gradually decreased to 92%, and remained relatively constant after 90 h on stream. The MBY conversion decreased from 49 to 42% during 100 h on stream. EDX analysis of the catalytic coating showed that the Pd content decreased from  $3.6 \pm 0.9$  to  $3.1 \pm 1.1$  wt.% and the Pd/Bi molar ratio increased from  $7.0 \pm 0.6$  to  $9.4 \pm 1.0$  after 100 h on stream. It is known that the partial blocking of Pd sites at higher Bi content decreases catalytic activity and at the same time it increases MBE selectivity [8,9,64]. Therefore it can be concluded that the decrease in activity was mainly caused by Pd leaching during hydrogenation reactions, while the increase in Pd/Bi ratio shows that the Bi leaching occurred to a larger extent than that of Pd.

It should be mentioned, the MBE selectivity and MBY conversion were constant during the first 5 h, and then the MBY conversion increased during a time-on-stream from 6 to 10 h at a constant MBE selectivity. These data suggest that during the first 5 h, Bi species leached from the multi-coordinated adsorption sites or from the catalyst support and no single Pd sites were liberated. It is known that these Bi species preferentially block step- and edge-sites of Pd nanoparticles that are the most active in MBY over-hydrogenation [8,9,48,65,66]. A steady decrease in selectivity in the period from 10 to 90 h on stream can be explained by the liberation of these Pd sites as a result of Bi leaching. Following the same reasoning, constant selectivity and an increase in activity during the period from 5 to 10 h can be explained by Bi leaching from more “selective” terrace sites. Finally, between 90 and 100 h on stream, selectivity was constant at about 92%. The EDX study of individual Pd nanoparticles showed that the Bi content was below the detection limit ( $\sim 0.1$  wt.%). A similar selectivity in MBY semihydrogenation reported over a Pd/TiO<sub>2</sub> catalyst [39] suggests that all Bi has been fully leached from the catalyst after 90 h. Some Bi observed in the sample after 100 h was likely attributed to Bi nanoparticles deposited on the support. TEM study of nanoparticles was attempted,

but no Bi particles were identified, likely, due to their very small dimensions, detection limit was around 1.5 nm for the system used.

There are three main possible mechanisms for Bi leaching from the Pd catalysts. Bi leaching from PdBi intermetallic compounds through the formation of Bi<sub>2</sub>O<sub>3</sub> was identified in electrochemical studies [67]. Segregation of bimetallic nanoparticles was demonstrated for a number of Pt- and Pd-based bimetallic catalysts in various reactions and may lead to leaching of Bi in the studied system [68–72]. Furthermore, a significant Bi leaching from Pd–Bi catalysts, observed in the selective oxidation of glyoxal and glucose, was associated with the formation of soluble chelate complexes of Bi [73,74].

Based on the existing data, it is difficult to identify the leaching mechanism realised in the studied system. However, a comparison of the MBY semihydrogenation under solvent-free conditions and in a non-polar hexane solution where no leaching was observed during 100 h [37] shows that leaching of Bi significantly depends on the polarity of solution. This suggests that the leaching was not caused by segregation because the latter process depends mainly on the nanoparticle composition rather than on solvent nature. Therefore the formation of Bi<sub>2</sub>O<sub>3</sub> and/or dissolution through the formation of chelate complexes are responsible for leaching.

It is known that oxidation of metallic Bi species can be suppressed in an acidic solution [51]. However, an acidic solution is unlikely to prevent leaching through complexation due to very high values of stability constants of chelate compounds [75,76]. Therefore the hydrogenation reaction was performed over the Pd–Bi/TiO<sub>2</sub> coating using a 1 vol.% acetic acid reactant solution to suppress the formation of Bi<sub>2</sub>O<sub>3</sub>.

Fig. 11 shows long-term MBY conversion and MBY selectivity data in the MBY hydrogenation over a Pd–Bi/TiO<sub>2</sub> catalyst in the presence of 1 vol.% acetic acid. It can be seen that a constant MBE selectivity of 98% was observed for 100 h on stream. The EDX data of the catalytic coating after the reaction showed the same Pd/Bi molar ratio ( $7.3 \pm 0.8$ ) as that in the fresh catalyst ( $7.0 \pm 0.6$ ). Therefore one can conclude that leaching of Bi in the solvent-free MBY hydrogenation was mainly caused by the formation of bismuth oxides or hydroxides by the reaction with the impurities in the initial solution such as dissolved oxygen or traces of water. For industrial applications, the acid introduced can be separated using conventional techniques as fractionation. Alternatively, in-flow separation can be performed using ion-exchange resins at the cost of below \$2 per kg of MBY feed [77–80]. The MBY conversion decreased by about 0.1% per hour and this deactivation did not depend on the acidity of the feedstock. It can be concluded that the primary reason of the catalyst deactivation was associated with the leaching of Pd. However, considering that during the test the amount of hydrogenated substrate was more than 105 times as high as the amount of Pd, the deactivation rate was remarkably low.

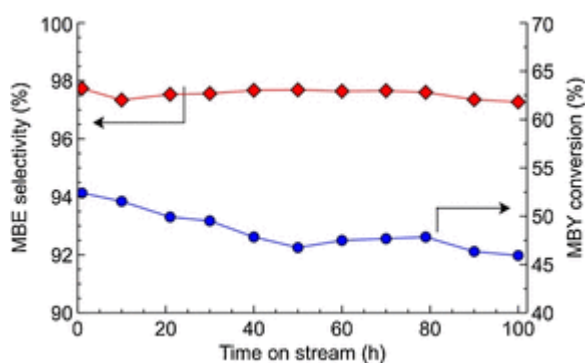


Fig. 11 MBY conversion and MBE selectivity over a Pd–Bi/TiO<sub>2</sub> coating in a 2 m capillary (0.53 mm i.d.) in the presence of 1 vol.% acetic acid. Liquid flow rate of 20  $\mu\text{L min}^{-1}$  and hydrogen flow of 5 mL  $\text{min}^{-1}$  (STP), 50 °C, ambient pressure, 0.2 bar pressure drop.

The operation of wall-coated capillary reactors under conditions when the active centre could perform the reaction cycle without being deactivated improves sustainability of the state-of-the-art semihydrogenation technology [15,22,25,26]. A comparison with solvent-free hydrogenation performed on Pd/ZnO and polymer-stabilised Pd nanoparticles shows similar maximum alkene yield of around 95% [61,81], while capillary reactor provides much better scalability due to the absence of heat transfer effects.

A throughput of 50 g  $\text{day}^{-1}$  exceeds the previously reported production rate by at least an order of magnitude and shows the feasibility of the capillary reactors for small-scale syntheses of fine chemicals. Process intensification by increasing the pressure within the reactor to at least 100 bar is expected to provide further throughput improvement by two orders of magnitude as the reaction has the first order in hydrogen pressure. Selective catalyst heating by radiofrequency or microwaves is expected to increase the throughput to the  $\sim 10$  kg  $\text{day}^{-1}$ , which is suitable for medium-scale high-value chemical syntheses [15,23]. Afterwards, the throughput can substantially be increased via numbering-up, i.e. increasing the number of capillaries and the length of capillaries bringing throughput to an order of at least 100 ton  $\text{year}^{-1}$  [82,83].

#### 4 Conclusions

Solvent-free semihydrogenation of 2-methyl-3-butyn-2-ol (MBY) was performed in 10 m long capillary reactors wall-coated with a Pd–Bi/TiO<sub>2</sub> catalyst. The highest MBE yield of 90% was achieved at 70 °C using the liquid flow rate of 40  $\mu\text{L min}^{-1}$  corresponding to a reactor throughput of 50 g  $\text{day}^{-1}$ . The addition of 10 mol.% pyridine to the reaction mixture increased the MBE yield to 95%, while it decreased the reactor throughput to 35 g  $\text{day}^{-1}$  due to a partial blockage of Pd active sites. The MBE selectivity was improved up to 98% by decreasing the Pd/Bi molar ratio in the bimetallic catalysts from 11 to 7. The leaching of Bi species via the formation of Bi oxides was responsible for a gradual decay in the MBE selectivity. However, the leaching was completely suppressed by addition of a 1 vol.% acetic acid solution to the MBY feed resulting in a stable operation for 100 h.

Another important conclusion is excellent reaction control achievable in capillary reactors. Capillary reactors provide the same semihydrogenation selectivity as the laboratory stirred tank batch reactors, where neither mass nor heat transfer limitations take place. As a result, selectivity towards intermediate reaction products in capillary reactors is determined by the nature of the system allowing for improved process safety, decreased labour costs and solvent consumption.

#### Acknowledgements

Authors are grateful to Dr. C. Wiles, Dr. M.G. Francesconi, Professor P. Fletcher and Professor B. Binks for the access to their equipment and to the European Commission for an FP7 Grant for the MAPSYN Project (MAPSYN.eu No. CP-IP 309376). The financial support provided by the European Research Council (ERC) project 279867 and the Russian Science Foundation project 15-13-20015 is gratefully acknowledged.

#### References

[1] W. Bonrath and T. Netscher, *Appl. Catal. A Gen.* 280, 2005, 55–73.

- [2] W. Bonrath, J. Medlock, J. Schutz, B. Wüstenberg and T. Netscher, In: I. Karame, (Ed), Hydrogenation, 2012, InTech; Rijeka, 69–90.
- [3] M. Eggersdorfer, D. Laudert, U. Létinois, T. McClymont, J. Medlock, T. Netscher and W. Bonrath, *Angew. Chem. Int. Ed.* 51, 2012, 12960–12990.
- [4] B. Chen, U. Dingerdissen, J.G.E. Krauter, H.G.J. Lansink Rotgerink, K. Möbus, D.J. Ostgard, P. Panster, T.H. Riermeier, S. Seebald, T. Tacke and H. Trauthwein, *Appl. Catal. A Gen.* 280, 2005, 17–46.
- [5] H.-U. Blaser, C. Malan, B. Pugin, F. Spindler, H. Steiner and M. Studer, *Adv. Synth. Catal.* 345, 2003, 103–151.
- [6] E.V. Rebrov, A. Berenguer-Murcia, H.E. Skelton, B.F.G. Johnson, A.E.H. Wheatley and J.C. Schouten, *Lab Chip* 9, 2009, 503–506.
- [7] A. Yarulin, I. Yuranov, F. Cardenas-Lizana, D.T.L. Alexander and L. Kiwi-minsker, *Appl. Catal. A Gen.* 478, 2014, 186–193.
- [8] J.A. Anderson, J. Mellor and R.K.P.K. Wells, *J. Catal.* 261, 2009, 208–216.
- [9] N. Cherkasov, A.O. Ibhadon, A. McCue, J.A. Anderson and S.K. Johnston, *Appl. Catal. A Gen.* 497, 2015, 22–30.
- [10] E. Esmaeili, A.M. Rashidi, A.A. Khodadadi, Y. Mortazavi and M. Rashidzadeh, *Fuel Process. Technol.* 120, 2014, 113–122.
- [11] M. Armbrüster, K. Kovnir, M. Behrens, D. Teschner, Y. Grin and R. Schlögl, *J. Am. Chem. Soc.* 132, 2010, 14745–14747.
- [12] D.M. Roberge, L. Ducry, N. Bieler, P. Cretton and B. Zimmermann, *Chem. Eng. Technol.* 28, 2005, 318–323.
- [13] L.N. Protasova, M. Bulut, D. Ormerod, A. Buekenhoudt, J. Berton and C.V. Stevens, *Org. Process Res. Dev.* 17, 2013, 760–791.
- [14] R.A. Sheldon, *Green Chem.* 16, 2014, 950–963.
- [15] V. Hessel, D. Kralisch, N. Kockmann, T. Noël and Q. Wang, *ChemSusChem* 6, 2013, 746–789.
- [16] C. Wiles and P. Watts, *Green Chem.* 14, 2012, 38–54.
- [17] I. Huerta, J. García-Serna and M.J. Cocero, *J. Supercrit. Fluids* 74, 2013, 80–88.
- [18] V. Paunovic, J.C. Schouten and T.A. Nijhuis, *Catal. Today* 248, 2015, 160–168.
- [19] K. Jähnisch, V. Hessel, H. Löwe and M. Baerns, *Angew. Chem. Int. Ed.* 43, 2004, 406–446.
- [20] W. Ehrfeld, V. Hessel and H. Löwe, *Microreactors*, 2000, Wiley-VCH Verlag GmbH & Co. KGaA; Weinheim, FRG.
- [21] K.F. Jensen, *Chem. Eng. Sci.* 56, 2001, 293–303.
- [22] M. Irfan, T.N. Glasnov and C.O. Kappe, *ChemSusChem* 4, 2011, 300–316.
- [23] V. Hessel, G. Cravotto, P. Fitzpatrick, B.S. Patil, J. Lang and W. Bonrath, *Chem. Eng. Process. Process Intensif.* 71, 2013, 19–30.

- [24] R.A. Skilton, A.J. Parrott, M.W. George, M. Poliakoff and R.A. Bourne, *Appl. Spectrosc.* 67, 2013, 1127–1131.
- [25] B.P. Mason, K.E. Price, J.L. Steinbacher, A.R. Bogdan and D.T. McQuade, *Chem. Rev.* 107, 2007, 2300–2318.
- [26] S.G. Newman and K.F. Jensen, *Green Chem.* 15, 2013, 1456–1472.
- [27] P. Watts and S.J. Haswell, *Chem. Eng. Technol.* 28, 2005, 290–301.
- [28] T. Noël, J.R. Naber, R.L. Hartman, J.P. McMullen, K.F. Jensen and S.L. Buchwald, *Chem. Sci.* 2, 2011, 287–290.
- [29] A.-K. Liedtke, F. Bornette, R. Philippe and C. de Bellefon, *Chem. Eng. J.* 227, 2013, 174–181.
- [30] T.A. Nijhuis, G. van Koten and J.A. Moulijn, *Appl. Catal. A Gen.* 238, 2003, 259–271.
- [31] M.W. Losey, M.A. Schmidt and K.F. Jensen, *Ind. Eng. Chem.* 40, 2001, 2555–2562.
- [32] S.K. Ajmera, M.W. Losey, K.F. Jensen and M.A. Schmidt, *AIChE J.* 47, 2001, 1639–1647.
- [33] R.B.N. Baig and R.S. Varma, *Chem. Commun.* 49, 2013, 752–770.
- [34] T.K. Houlding and E.V. Rebrov, *Green Process. Synth.* 1, 2012, 19–31.
- [35] L.M. Rossi, N.J.S. Costa, F.P. Silva and R. Wojcieszak, *Green Chem.* 16, 2014, 2906–3380.
- [36] T. Zhang, X. Zhang, X. Yan, L. Kong, G. Zhang, H. Liu, J. Qiu and K.L. Yeung, *Chem. Eng. J.* 228, 2013, 398–404.
- [37] N. Cherkasov, A.O. Ibhaden and E.V. Rebrov, *Lab Chip* 15, 2015, 1952–1960.
- [38] M. Faustini, B. Louis, P.A. Albouy, M. Kuemmel and D. Grosso, *J. Phys. Chem. C* 114, 2010, 7637–7645.
- [39] E.V. Rebrov, E.A. Klinger, A. Berenguer-Murcia, E.M. Sulman and J.C. Schouten, *Org. Process Res. Dev.* 13, 2009, 991–998.
- [40] L.N. Protasova, E.V. Rebrov, H.E. Skelton, A.E.H. Wheatley and J.C. Schouten, *Appl. Catal. A Gen.* 399, 2011, 12–21.
- [41] C.H. Hornung, B. Hallmark, M.R. Mackley, I.R. Baxendale and S.V. Ley, *Adv. Synth. Catal.* 352, 2010, 1736–1745.
- [42] B.H. Alsolami, R.J. Berger, M. Makkee and J.A. Moulijn, *Ind. Eng. Chem. Res.* 52, 2013, 9069–9085.
- [43] D. van Herk, P. Castaño, M. Makkee, J.A. Moulijn and M.T. Kreutzer, *Appl. Catal. A Gen.* 365, 2009, 199–206.
- [44] B.A. Wilhite, R. Wu, X. Huang, M.J. McCready and A. Varma, *AIChE J.* 47, 2001, 2548–2556.
- [45] J.J.W. Bakker, M.M.P. Zieverink, R.W.E.G. Reintjens, F. Kapteijn, J.A. Moulijn and M.T. Kreutzer, *ChemCatChem* 3, 2011, 1155–1157.
- [46] M. Ueno, T. Suzuki, T. Naito, H. Oyamada and S. Kobayashi, *Chem. Commun.* 2008, 1647–1649.

- [47] J. Kobayashi, Y. Mori, K. Okamoto, R. Akiyama, M. Ueno, T. Kitamori and S. Kobayashi, *Science* 304, 2004, 1305–1308.
- [48] J.A. Bennett, G.A. Attard, K. Deplanche, M. Casadesus, S.E. Huxter, L.E. Macaskie and J. Wood, *ACS Catal.* 2, 2012, 504–511.
- [49] R. Bleta, P. Alphonse and L. Lorenzato, *J. Phys. Chem. C* 114, 2010, 2039–2048.
- [50] L. Liu and X. Chen, *Chem. Rev.* 114, 2014, 9890–9918.
- [51] A. Economou, *TrAC Trends Anal. Chem.* 24, 2005, 334–340.
- [52] T.V. Nghi and F. Vydra, *J. Electroanal. Chem. Interfacial Electrochem.* 71, 1976, 325–332.
- [53] J. Yue, G. Chen, Q. Yuan, L. Luo and Y. Gonthier, *Chem. Eng. Sci.* 62, 2007, 2096–2108.
- [54] P. Sobieszuk, J. Aubin and R. Pohorecki, *Chem. Eng. Technol.* 35, 2012, 1346–1358.
- [55] A. Günther, S.A. Khan, M. Thalmann, F. Trachel and K.F. Jensen, *Lab Chip* 4, 2004, 278–286.
- [56] D. Mei, P. Sheth, M. Neurock and C. Smith, *J. Catal.* 242, 2006, 1–15.
- [57] G. Wowsnick, D. Teschner, M. Armbrüster, I. Kasatkin, F. Girgsdies, Y. Grin, R. Schlögl and M. Behrens, *J. Catal.* 309, 2014, 221–230.
- [58] V. van Steijn, M.T. Kreutzer and C.R. Kleijn, *Chem. Eng. J.* 135, 2008, S159–S165.
- [59] M. García-Mota, J. Gómez-Díaz, G. Novell-Leruth, C. Vargas-Fuentes, L. Bellarosa, B. Bridier, J. Pérez-Ramírez and N. López, *Theor. Chem. Acc.* 128, 2010, 663–673.
- [60] M. García-Mota, J. Gómez-Díaz, G. Novell-Leruth, C. Vargas-Fuentes, L. Bellarosa, B. Bridier, J. Pérez-Ramírez and N. López, *Theor. Chem. Acc.* 128, 2011, 663–673.
- [61] M. Crespo-Quesada, M. Grasemann, N. Semagina, A. Renken and L. Kiwi-Minsker, *Catal. Today* 147, 2009, 247–254.
- [62] N. Semagina, M. Grasemann, N. Xanthopoulos, A. Renken and L. Kiwi-Minsker, *J. Catal.* 251, 2007, 213–222.
- [63] D. Duca, L.F. Liotta and G. Deganello, *J. Catal.* 154, 1995, 69–79.
- [64] J. Sá, J. Montero, E. Duncan and J.A. Anderson, *Appl. Catal. B Environ.* 73, 2007, 98–105.
- [65] M. Crespo-Quesada, A. Yarulin, M. Jin, Y. Xia and L. Kiwi-Minsker, *J. Am. Chem. Soc.* 133, 2011, 12787–12794.
- [66] E. Herrero, V. Climent and J.M. Feliu, *Electrochem. Commun.* 2, 2000, 636–640.
- [67] D.R. Blasini, D. Rochefort, E. Fachini, L.R. Alden, F.J. DiSalvo, C.R. Cabrera and H.D. Abruña, *Surf. Sci.* 600, 2006, 2670–2680.
- [68] K.J.J. Mayrhofer, K. Hartl, V. Juhart and M. Arenz, *J. Am. Chem. Soc.* 131, 2009, 16348–16349.
- [69] S. Gonzalez, K.M. Neyman, S. Shaikhutdinov, H.-J. Freund and F. Illas, *J. Phys. Chem. C* 2, 2007, 6852–6856.
- [70] O.M. Løvvik, *Surf. Sci.* 583, 2005, 100–106.

- [71] J.L. Rousset, J.C. Bertolini and P. Miegge, *Phys. Rev. B* 53, 1996, 4947–4957.
- [72] N. López and C. Vargas-Fuentes, *Chem. Commun.* 48, 2012, 1379–1391.
- [73] M. Wenkin, P. Ruiz, B. Delmon and M. Devillers, *J. Mol. Catal. A Chem.* 180, 2002, 141–159.
- [74] F. Alardin, B. Delmon, P. Ruiz and M. Devillers, *Catal. Today* 61, 2000, 255–262.
- [75] W.R. Harris, Y. Chen, J. Stenback and B. Shah, *J. Coord. Chem.* 23, 1991, 173–186.
- [76] A.A. Frutos, L.F. Sala, G.M. Escandar, M. Devillers, J.M. Salas Peregrín and M. González Sierra, *Polyhedron* 18, 1999, 989–994.
- [77] H.M. Anasthas and V.G. Gaikar, *Sep. Sci. Technol.* 36, 2001, 2623–2646.
- [78] G.M. Gusler, T.E. Browne and Y. Cohen, *Ind. Eng. Chem. Res.* 32, 1993, 2727–2735.
- [79] Y.K. Hong and W.H. Hong, *Sep. Purif. Technol.* 42, 2005, 151–157.
- [80] H.M. Anasthas and V.G. Gaikar, *React. Funct. Polym.* 47, 2001, 23–35.
- [81] N. Semagina, A. Renken, D. Laub and L. Kiwi-Minsker, *J. Catal.* 246, 2007, 308–314.
- [82] M. Al-Rawashdeh, F. Yue, N.G. Patil, T.A. Nijhuis, V. Hessel, J.C. Schouten and E.V. Rebrov, *AIChE J.* 60, 2014, 1941–1952.
- [83] M. Al-Rawashdeh, F. Yu, T.A. Nijhuis, E.V. Rebrov, V. Hessel and J.C. Schouten, *Chem. Eng. J.* 207–208, 2012, 645–655.